Article

Interannual Variation in the Zooplankton Community of the North Adriatic Sea under Short-Term Climatic Anomalies

Samuele Menicucci [1,2], Andrea De Felice [1], Ilaria Biagiotti [1], Giovanni Canduci [1], Ilaria Costantini [1], Antonio Palermino [1], Michele Centurelli [1] and Iole Leonori [1,*]

[1] National Research Council (CNR), IRBIM-Institute for Marine Biological Resources and Biotechnology, Largo Fiera della Pesca, 2, 60125 Ancona, Italy; samuele.menicucci@irbim.cnr.it (S.M.); andrea.defelice@cnr.it (A.D.F.); ilaria.biagiotti@cnr.it (I.B.); giovanni.canduci@cnr.it (G.C.); ilaria.costantini@cnr.it (I.C.); antonio.palermino@irbim.cnr.it (A.P.); michele.centurelli@irbim.cnr.it (M.C.)

[2] Alma Mater Studiorum, Department of Biological, Geological and Environmental Sciences (BiGeA), University of Bologna, Via Zamboni, 33, 40126 Bologna, Italy

* Correspondence: iole.leonori@cnr.it

Abstract: Zooplankton are a pivotal component of the pelagic community, and their abundance and distribution are often strongly dependent on environmental conditions at sea. However, climate change can pose significant challenges to planktonic organisms. Therefore, in this study, we tried to address the possible effect of short-term climatic anomalies on the zooplankton community in the North Adriatic Sea, comparing mesozooplankton composition in June between two years with very different temperature and rainfall levels, i.e., 2019 and 2022. Environmental conditions at sea were significantly different, since 2022 faced rising temperatures in the northern part of the area and higher salinity and lower chlorophyll values in coastal samples. Our data unveiled a community shift, from a *Noctiluca*-dominated community to a crustacean-dominated one, and revealed that even offshore areas can be subject to changes, despite having quite stable environmental parameters. Our findings confirmed the influence of river inputs and temperature on the Adriatic community's distribution and composition, highlighting how climate-driven changes could have unpredictable effects on the whole Adriatic ecosystem. Indeed, each species has its own role in ecosystem functioning and climatic anomalies could uncouple the fine-scale connections that make up the pelagic trophic web.

Keywords: Adriatic Sea; zooplankton; climate change; MEDIAS; ecology; copepods; cladocerans; *Noctiluca scintillans*

1. Introduction

Zooplankton are an extremely diverse group, with sizes ranging from 2 μm for nanozooplankton to more than 200 mm for megazooplankton [1]. Zooplankton are also extremely abundant, with a biomass that encompasses about 40% of the total pelagic biomass. Half of that is represented by mesozooplankton, that is the fraction between 200 and 2000 μm [2]. Zooplankton are a key component of pelagic marine ecosystems, as they act as a link between primary producers and higher-order predators [3], from carnivorous zooplankters and larvae of larger fishes [4] to small pelagic fishes and large oceanic filter feeders [5,6]. Moreover, zooplankton can also contribute to the regeneration of nitrogen for microbes and phytoplankton through excretion [7] and connect the microbial loop to the "canonical" food web through predation on nanoplankton [8]. Finally, fecal pellets and dead zooplankton sink to the bottom, where a fraction is captured by benthic fauna, contributing to the enrichment of the seafloor [9]; the rest is buried in the sediment, acting as a sink for CO_2 [10]. Such properties, usually regarded as "ecosystem services", are determined by the functional traits of the organisms in the community. The composition and abundance of this planktonic community are strongly influenced by environmental conditions and

bottom-up mechanisms; therefore, studying how climatic anomalies can alter their features is fundamental to preserving ecosystem functioning and trophic coupling [3].

The Adriatic Sea is a semi-enclosed basin that exchanges water with the Mediterranean Sea through the Strait of Otranto at its southern boundary. The North Adriatic is a shallow sea, with a mean depth of about 30 m, characterized by colder waters and high river inputs, while the southern part is warmer and saltier, reaching a maximum depth of 1270 m [11]. The large extent of the continental platform and high nutrient input from coastal areas make the Adriatic Sea the most productive basin of the Mediterranean [12]. The cooler area in the north represents a suitable habitat for boreal species like *Merlangius merlangus* (Linnaeus, 1758), *Sprattus sprattus* (Linnaeus, 1758), *Fucus virsoides* (J.Agardh, 1868) and *Pseudocalanus elongatus* (Brady, 1865) [13,14].

However, the Adriatic is also one of the most vulnerable areas to climate change, facing the largest increases in temperature [15,16]. Such conditions can be extremely harmful for cold-water species, as they would be trapped in a cul-de-sac with no way out to a colder sea [17,18]. Moreover, temperature is not the only aspect affected by climate change; many authors have registered a negative trend in precipitation in Mediterranean countries, with a more severe toll for the Adriatic in winter, spring, and summer [16,19–21]. This anomaly has negative returns for the hydrological conditions of the Po River, which faces more frequent and more alarming droughts [16,22]. The Po River is the main contributor to the Adriatic's freshwater input; therefore, a severe reduction in its flow is expected to greatly affect the oceanographic conditions of the whole basin [16,23–25].

At the start of 2022, seven months of scarce precipitation led to a reduction in rain and snowmelt, causing a decrease in river flow that was 30% higher than the previous record (Figure 1). This severe and prolonged drought in Northern Italy sparked serious concerns over the socioeconomic impact on agriculture, industry, and energy production [26]. This year was also extremely hot, being the second warmest for Europe and 0.85 °C above the average for the 1991–2020 reference period. Heatwaves are indeed becoming stronger and more common each year, posing a serious threat to both human health and marine life [27,28].
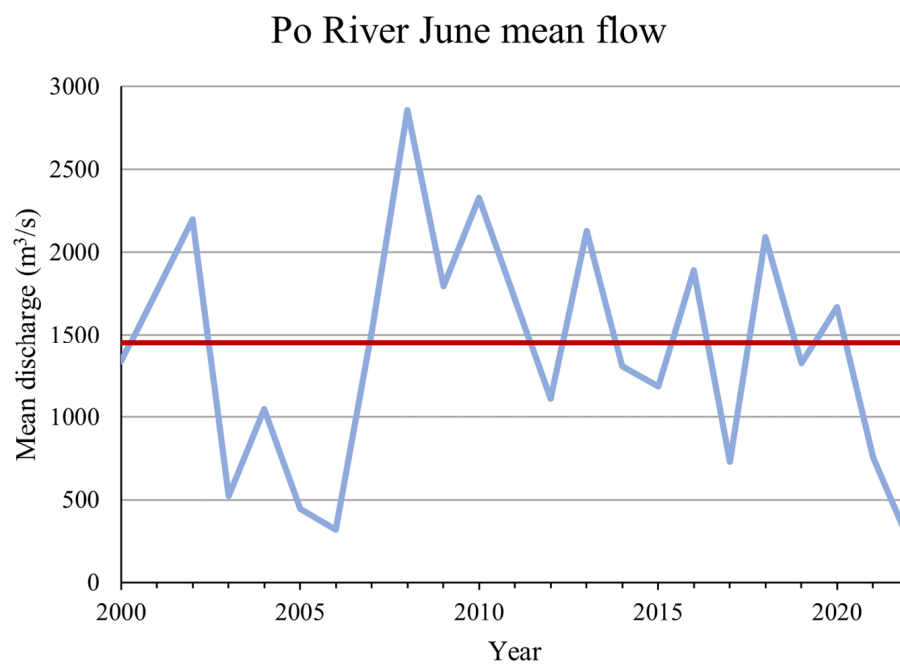
Po River June mean flow

Figure 1. Monthly mean discharge (in $m^3 s^{-1}$) of the Po River at Pontelagoscuro, Italy in June from 2000 to 2022. The red line is the mean discharge in June averaged over the whole period. Data were sourced from [29].

In this context of extreme climatic distress, we tried to address changes in the pelagic community, comparing the diversity of mesozooplankton in the North Adriatic Sea between June 2019, which has been a colder and much rainier year, and June 2022, characterized by extreme heat and water deficit. We also investigated how the extreme draught and the high temperatures shaped the 2022 pelagic environment, trying to link changes in abiotic parameters with shifts in plankton composition. Plankton and climate change monitoring can provide crucial information on the status of pelagic habitats and environmentally driven fish productivity, linking fish stock fluctuations and variations in lower trophic levels, which is a clear step towards the recommended ecosystem-based management of fish stocks [30].

2. Materials and Methods

2.1. Study Area

The Adriatic Sea is a semi-enclosed basin that extends between the Italian and the Balkan Peninsula, with its major axis (about 800 km versus 200 km) in a NW–SE direction (Figure 2). It is usually divided into three sub-basins, according to their bathymetry profile. The North Adriatic is very shallow, with a mean depth of about 30 m, and is characterized by high river inputs, which favor a rich primary production. The main contributor is the Po River, which provides about 28% of the total freshwater input and 50% of the external nutrient input of the whole Adriatic [31,32]. The middle Adriatic is a transition zone between northern and southern sub-basins, with the two Jabuka (Pomo) depressions reaching 270 m depth. The southern sub-basin is characterized by a wide depression that is about 1270 m in depth. Here, the Otranto channel allows limited water exchange with the Mediterranean Sea [12]. The Adriatic is a temperate warm sea, with temperatures ranging from 6° in winter to 29 °C in summer and only rarely dropping below 10 °C, even in the deeper layers. A general increase in temperature from north to south can be observed in winter, while temperatures are more uniform in other seasons [12]. A clear gradient in salinity can also be observed from north to south and from inshore to offshore areas, but with some seasonal differences: the 38.0 PSU isohaline is located near the coast during winter, while during spring and summer, it spreads southward and offshore thanks to an increased thermal stratification [11].

There are three principal water masses in the Adriatic Sea: the Adriatic Surface Water (AdSW), the Levantine Intermediate Water (LIW), and the Adriatic Deep Water (AdDW) (with every sub-basin having its own characteristic deep water). The LIW is a high-salinity water that forms in the Levantine basin and is partially diluted along its way to the Ionian Sea, where it can enter the Adriatic through the Otranto Channel. The NAdDW (Northern Adriatic Deep Water), characterized by a very low temperature, relatively low salinity, and high density, is formed in the northern basin during winter, when the strong Bora wind causes evaporation and cooling of surface waters. The NAdDW can fill up the Jabuka/Pomo Pit and occasionally spreads to the South Adriatic. The MAdDW (Middle Adriatic Deep Water) is formed in Jabuka/Pomo Pit, when there is limited Mediterranean water inflow. The SAdDW (Southern Adriatic Deep Water) originates in the Southern Adriatic Pit and spreads into the bottom layer of the Eastern Mediterranean [11,12]. The general circulation is cyclonic with a flow towards the northwest along the eastern side and a return flow towards the southeast along the western side. The circulation in the three sub-basins is often dominated by their own cyclonic gyres, which vary in intensity according to the season. The sub-gyre of the southern Adriatic tends to persist throughout the year. The sub-gyre of the middle Adriatic is more pronounced in summer and autumn, while in the north, a cyclonic gyre is evident in front of the Po River mouth only in autumn [11].
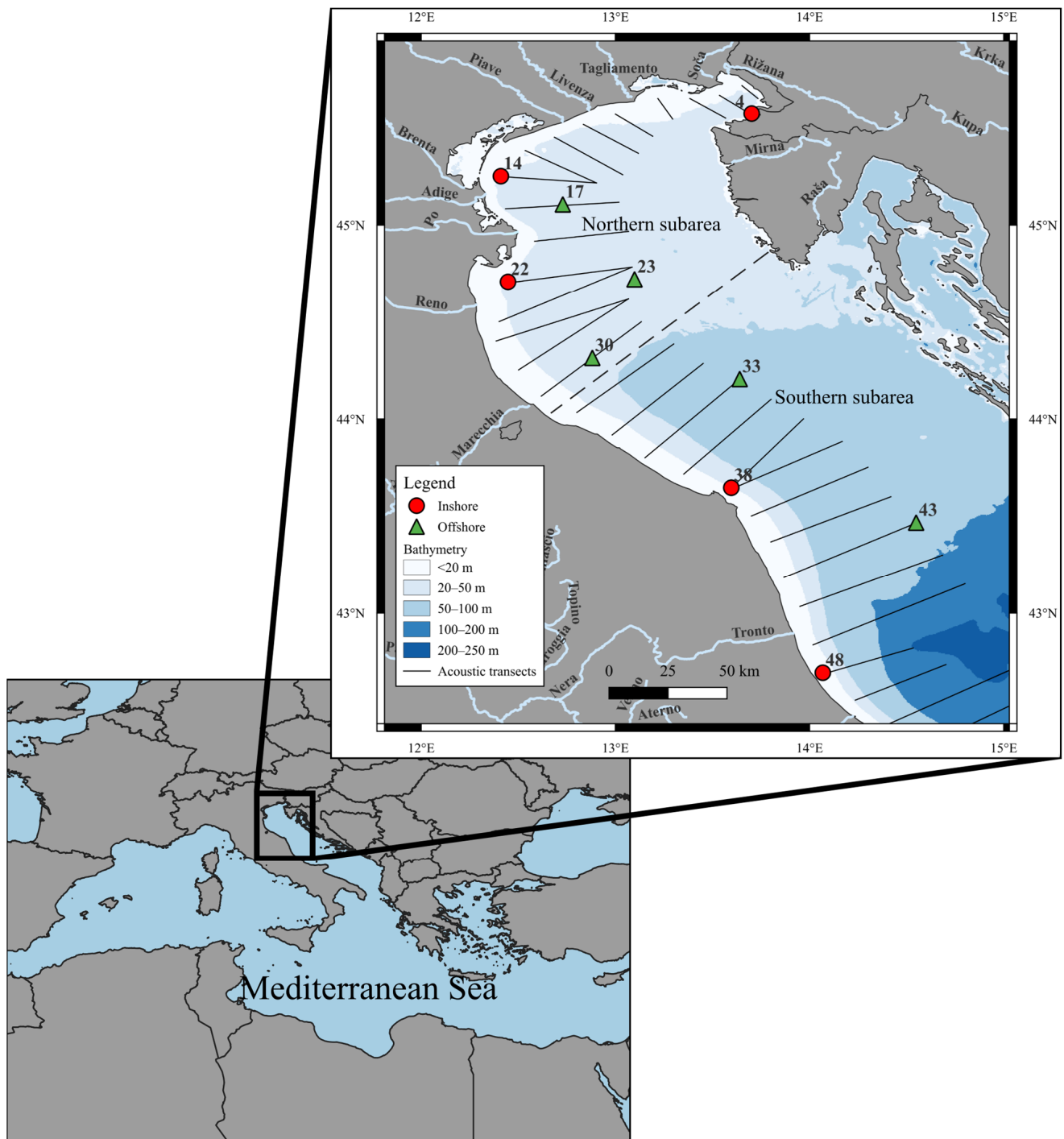
Figure 2. Map of the Mediterranean Sea with a close-up of the Adriatic Sea showing the position of the sampling stations.

The North Adriatic Sea is a very productive area due to the presence of large river inputs and a wide continental platform that favors a shorter trophic chain and faster energy transfer [12]. Phytoplankton biomass usually reaches its maximum in spring, with a second peak in autumn, following the same pattern observed in river discharge [33,34]. As a result, zooplankton reach their maximum abundance in summer, when the mesozooplankton community is usually dominated by copepods, cladocerans, doliolids, *Noctiluca scintillans*, siphonophores, and larvae of invertebrates [35–37].

These characteristics determine the presence of a very valuable fishing industry, mainly focused on small pelagic fishes and demersal species [38]. However, in recent years, eutrophication from river discharge has also been associated with recurring mucilage events, algal blooms, and hypoxia, which can cause the suffering of benthic communities [39,40].

2.2. Sample Collection and Analysis

Samples for this study were collected onboard the R/V "G. Dallaporta" during the MEDIAS 2019 and MEDIAS 2022 acoustic surveys that took place in June in the western side of the Northern Adriatic Sea [41]. MEDIAS (MEDiterranean International Acoustic Surveys) Steering Committee coordinates among participant countries the acoustic surveys performed in the Mediterranean and Black Sea to assess the biomass and spatial distribution of small pelagic fish using both acoustic and biological fish data [41,42]. However, acoustic surveys can also collect data on other pelagic components, for a better evaluation of the processes that determine pelagic fish dynamics [41,43].

Zooplankton samples were collected through a 2.6 m long WP2 net with a 200 μm mesh size and a circular mouth with a 57 cm diameter. Vertical tows were performed with a towing speed of $1 \, \text{m s}^{-1}$, starting from 3 m above the bottom, to the surface. Sampling stations were located along acoustic transects. In 2019, most of the sampling was performed during the night, while in 2022, all samples were collected during the day. Sampled organisms were then preserved in 4% buffered formaldehyde. Environmental data at each station were also collected through a SBE 911plus CTD, recording pressure (dbar, decibar), temperature (°C), fluorescence (as a proxy for phytoplankton biomass, expressed as $\mu\text{g L}^{-1}$), dissolved oxygen (expressed as mL L^{-1} and saturation percentage), salinity (PSU), and density (kg m^{-3}). Sampling stations in the study area were divided according to their distance from the coast in inshore and offshore stations. Moreover, the sampling area was divided according to the bathymetric profile into a northern part, reaching up to 50 m depth, and a southern part, up to 100 m depth (Figure 2).

Ten zooplankton samples for each year were analyzed to characterize the planktonic community. Samples were selected from both coastal and open sea areas, encompassing different bathymetric profiles up to 100 m depth. The whole sample was rinsed and filtered with a 200 μm sieve, and the obtained mass was weighed (wet weight, WW, in g, precision 10^{-4}). Then, samples were quickly sorted to isolate, identify, and count larger and less abundant organisms. About 1/20th of the sample was then weighed, and all organisms in the sub-sample were identified to the lowest taxonomic level possible under a stereomicroscope before being counted.

2.3. Statistical Analysis

We first tried to compare the environmental variables of investigated years to assess whether the climatic anomaly of 2022 actually influenced the environmental conditions at sea. Therefore, data of salinity, temperature, oxygen saturation, and fluorescence were averaged across the whole water column and plotted in a draftsman's plot to assess the skewness of the variables; temperature and fluorescence were log(x + 1)-transformed to fit a linear distribution. The matrix of environmental variables was then normalized to perform the principal component analysis (PCA), which is an ordination in which samples are projected onto a "best-fitting" plane, capturing as much of the variability as possible [44]. The same matrix was also used for a hierarchical cluster analysis (average grouping method), to group samples according to homogeneous variables. Finally, a three-way univariate PERMANOVA (permutational multivariate analysis of variance, [45]), with factors described in Table 1, was used on the Euclidean distance matrix of salinity, oxygen saturation, log(x + 1)-temperature, and log(x + 1)-fluorescence to test the presence and significance of both spatial and temporal differences. This test was run under 9999 permutations, with permutation of residuals under a reduced model as the permutation method; significant p values were set at $p < 0.05$. In the case of a significant difference in the interaction of "factor"

year with either "sub-area" or "in–offshore", a pairwise comparison was also performed to test differences at a finer scale.

Table 1. Factors used for the PERMANOVA tests on environmental variables and biological data.

Factors	Levels	Fixed/Random
Year	2019/2022	Fixed
Sub-area	North/South	Fixed
In-offshore	Inshore/offshore	Fixed

Abundance data obtained from the samples analysis were standardized to the sampled area to avoid dilution in a large water volume for deeper stations. For each station, the Shannon–Wiener (H′) diversity index was calculated. Then, total biomass, total abundance, and the H′ diversity index were tested by univariate PERMANOVA analyses. Tests were run on Euclidean distance resemblance matrixes of log(x + 1)-transformed data for abundance, biomass, and H′ values and using the same design and method applied for environmental variables.

A new PERMANOVA test was performed on the Bray–Curtis resemblance matrix of log(x + 1)-transformed abundance zooplankton data, using the same design described for previous analyses, to assess the presence and significance of variations in the zooplanktonic community. Transformation is usually applied to assemblage matrices of abundance to downweight the contributions of quantitatively dominant species to the similarities calculated between samples. This is particularly important for Bray–Curtis similarity, which does not incorporate any form of scaling of each species by its total or maximum across all samples. The more severe the initial transformation, the more notice is taken of the less abundant species in the matrix. To take notice also of the less abundant species and compress the contribution from dominant species, a log(x + 1) transformation was employed in this analysis [45]. The same resemblance matrix was also used to perform a non-metric multi-dimensional scaling (nMDS). Its purpose is to represent the samples as points in a bidimensional space, such that the relative distances apart of all points are in the same rank order as the relative dissimilarities of the samples [44]. Samples were also grouped through a hierarchical cluster analysis (average grouping method) to assess the level of similarity for identified associations.

A SIMPER (similarity percentages) analysis was carried out according to the same sampling design to identify the most typifying taxon contributing to the average similarity/dissimilarity among the examined years [44]. This was conducted using Bray–Curtis similarity, with a cut-off for low contribution at 50%.

To identify the environmental drivers of zooplanktonic communities and their structure across the sampling area, biotic data were correlated with environmental variables. Environmental data were tested for collinearity among variables by using a draftsman's plot, with fluorescence and temperature being log(x + 1)-transformed to fit a linear distribution in the draftsman's plot. This step is necessary to run a parsimonious model without redundancies. Afterward, a DistLM (distance-based linear models, [45]) was run with temperature and salinity as environmental variables, using "step-wise" as the selection procedure and "AIC (Akaike Information Criterion)" as the selection criterion. All statistical analyses were run using PERMANOVA+ for PRIMER 6 software [44,45].

Finally, to assess the correlation of the most abundant groups of zooplankton with environmental variables, Spearman's correlation was run using the rcorr function in the hmisc package on R 4.3.2 (https://www.r-project.org, R Core Team, accessed on 15 December 2023). The biological data used were log(x + 1)-transformed data of abundance for *Noctiluca scintillans*, Cladocera, Copepoda, Thaliacea, total abundance, total biomass, species richness, and H' index, with untransformed values of salinity and the log(x + 1)-transformed data of temperature as environmental variables.

3. Results

3.1. Influence of Climatic Anomalies on Environmental Variables

The PCA of environmental variables (Figure 3a) unveiled that samples from 2022 in general had higher temperature and salinity values. Said differences appeared more evident in inshore stations, which had a much more scattered distribution than offshore stations. Results from the cluster analysis (Figure 3b) confirmed the interannual continuity of offshore samples, which were grouped together, while coastal samples were divided into two different branches: (i) northern inshore samples from 2019 and (ii) northern inshore samples from 2022 and southern inshore samples from both years. Station 48_2019 was isolated from other samples as it had much higher temperature values. Univariate PERMANOVA analyses on the environmental variables (Table S1 in Supplementary Materials) revealed that only fluorescence and salinity showed significant variation between the examined years; from the pairwise tests, we were able to determine that, for both variables, the difference was only significant for inshore stations. Since only the interaction of terms "year" and "sub-area" showed significant variation in temperature, we performed a pairwise test to assess significance at a finer scale, revealing that such difference was only significant in the northern sub-area.

3.2. Changes in the Mesozooplankton Community

Analysis of biological samples did not reveal significant variations in abundance, biomass, and H' index between 2019 and 2022 over the whole area (Figures 4 and 5). However, a significant increase between the examined years was found for H' values in the northern sub-area thanks to the pairwise test. Species richness, on the other hand, decreased from 2019 to 2022, with the pairwise test indicating that such variation was significant only in the southern sub-area (Table S2 in Supplementary Materials).

In samples from 2019 (Table S6 in Supplementary Materials), the dominant species was the heterotrophic dinoflagellate *Noctiluca scintillans*, which represented up to 97% of total abundance (Figure 5a). Copepods were the most abundant crustaceans in all stations, with *Acartia* sp., *Oithona* sp., and small unidentified calanoids as the dominant taxa. Large copepods were much less abundant, especially in northern stations, and mainly represented by *Calanus helgolandicus*, *Centropages typicus*, *Paraeuchaeta hebes*, and *Temora stylifera*. The invasive copepod *Pseudodiaptomus marinus* was also abundant in station 48. Cladocerans were the second most abundant group for crustaceans, with *Pleopis polyphemoides*, *Penilia avirostris*, and *Evadne spinifera* as the most common species. Gelatinous zooplankton was locally abundant in offshore stations of the southern area, mainly represented by the small doliolid *Doliolina muelleri*. Other abundant taxa were *Oikopleura* sp., *Muggiaea* sp., anthomedusae, and Chaetognatha. Meroplankton was mostly present as veliger larvae of bivalves and gastropods, ophioplutei, decapod zoeae, and anchovy eggs and larvae (Figure 6).
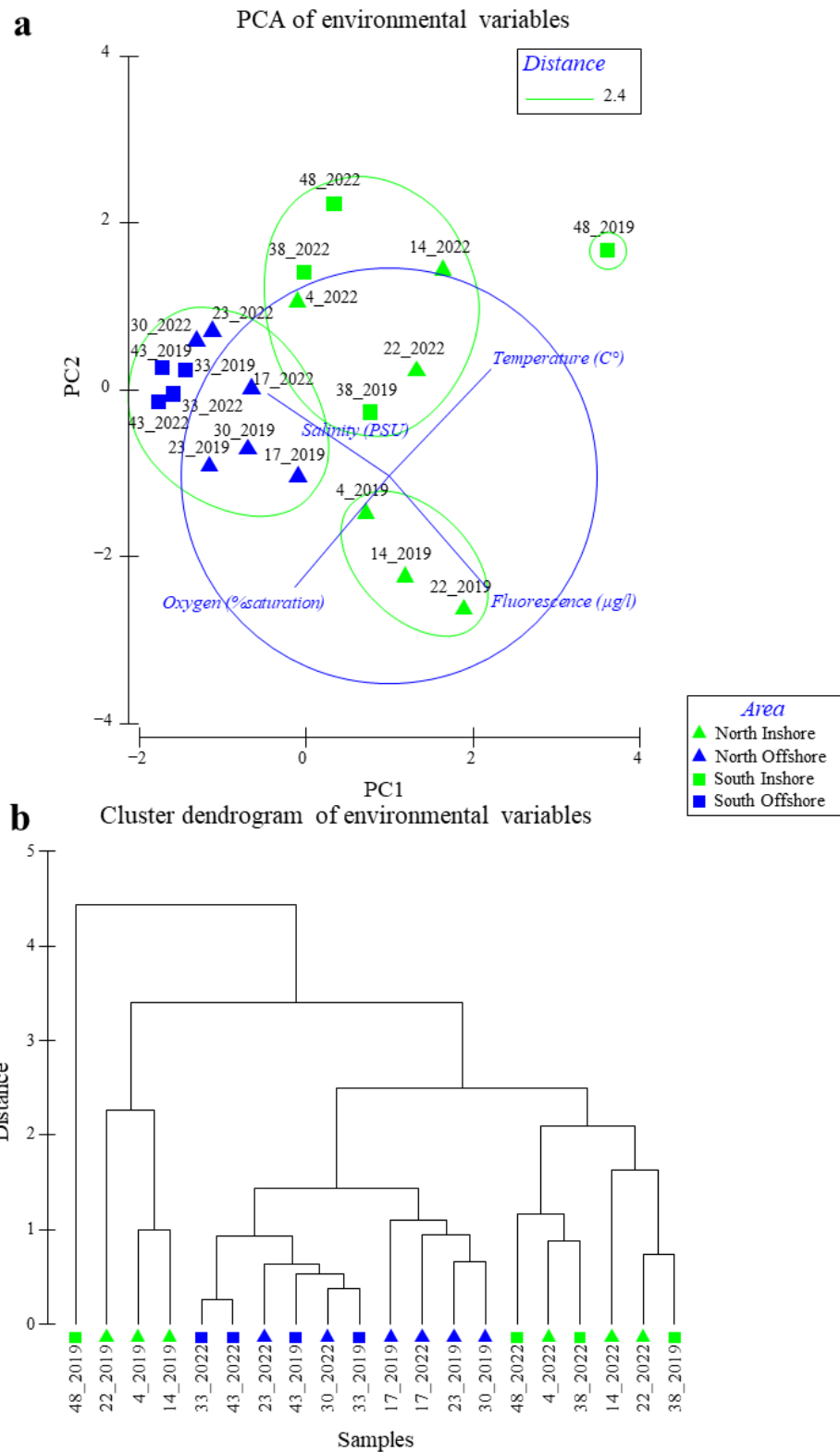
Figure 3. Results from the (**a**) PCA analysis and (**b**) hierarchical cluster analysis performed on the multivariate matrix of the environmental variables registered during the survey. The vector length reflects the importance of that variable's contribution to these particular two PC axes in relation to all possible PC axes. PC1 explained 52.2% of variation, while PC2 explained 40.3% of variation. The overlayed clusters in (**a**) are groups identified by (**b**) at 2.4 Euclidean distance.
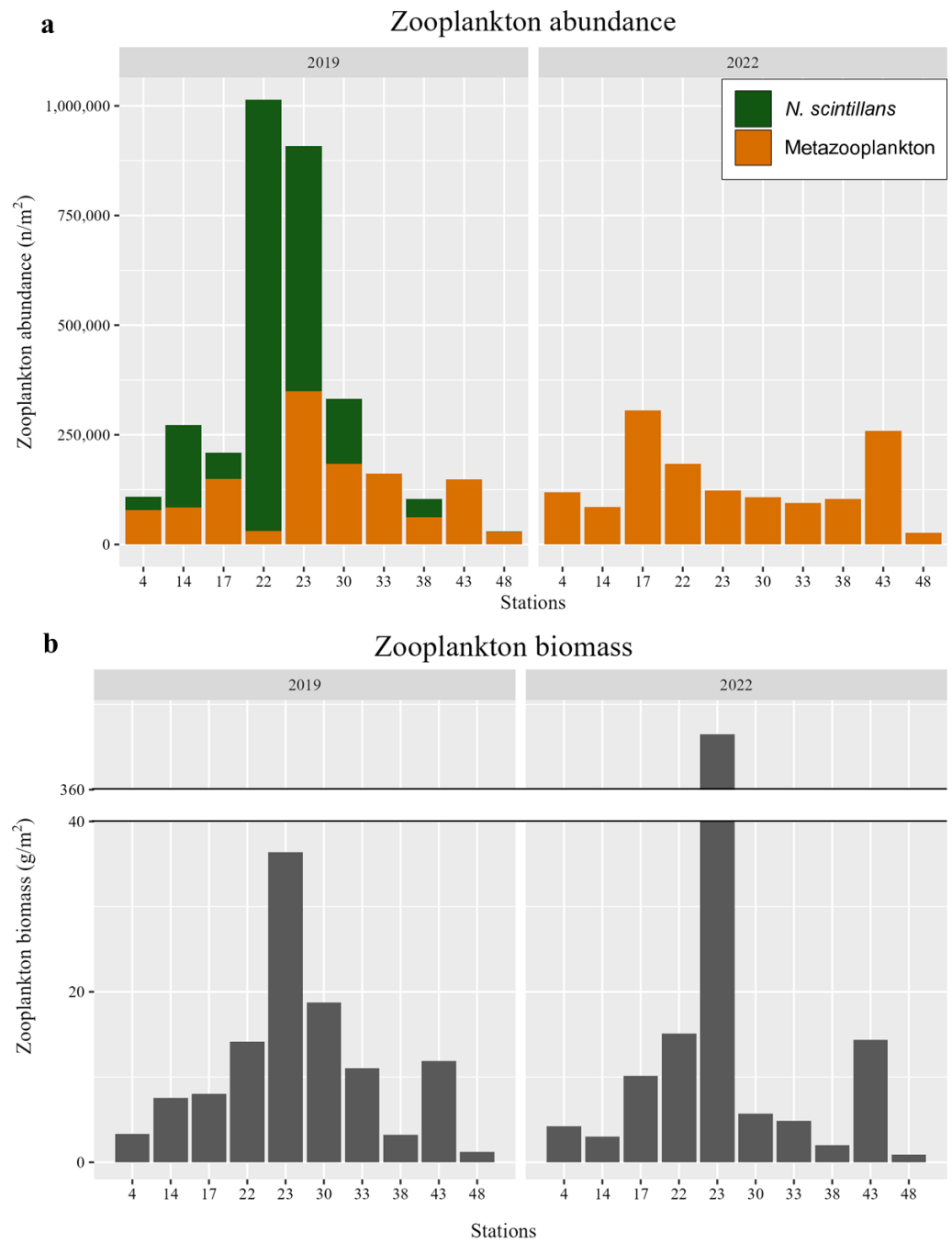
Figure 4. Results from the analysis of zooplankton samples from 2019 and 2022: (**a**) bar plot of abundance values, expressed as individuals per m^2; (**b**) bar plot of the biomass of examined samples, expressed as g m^{-2}.
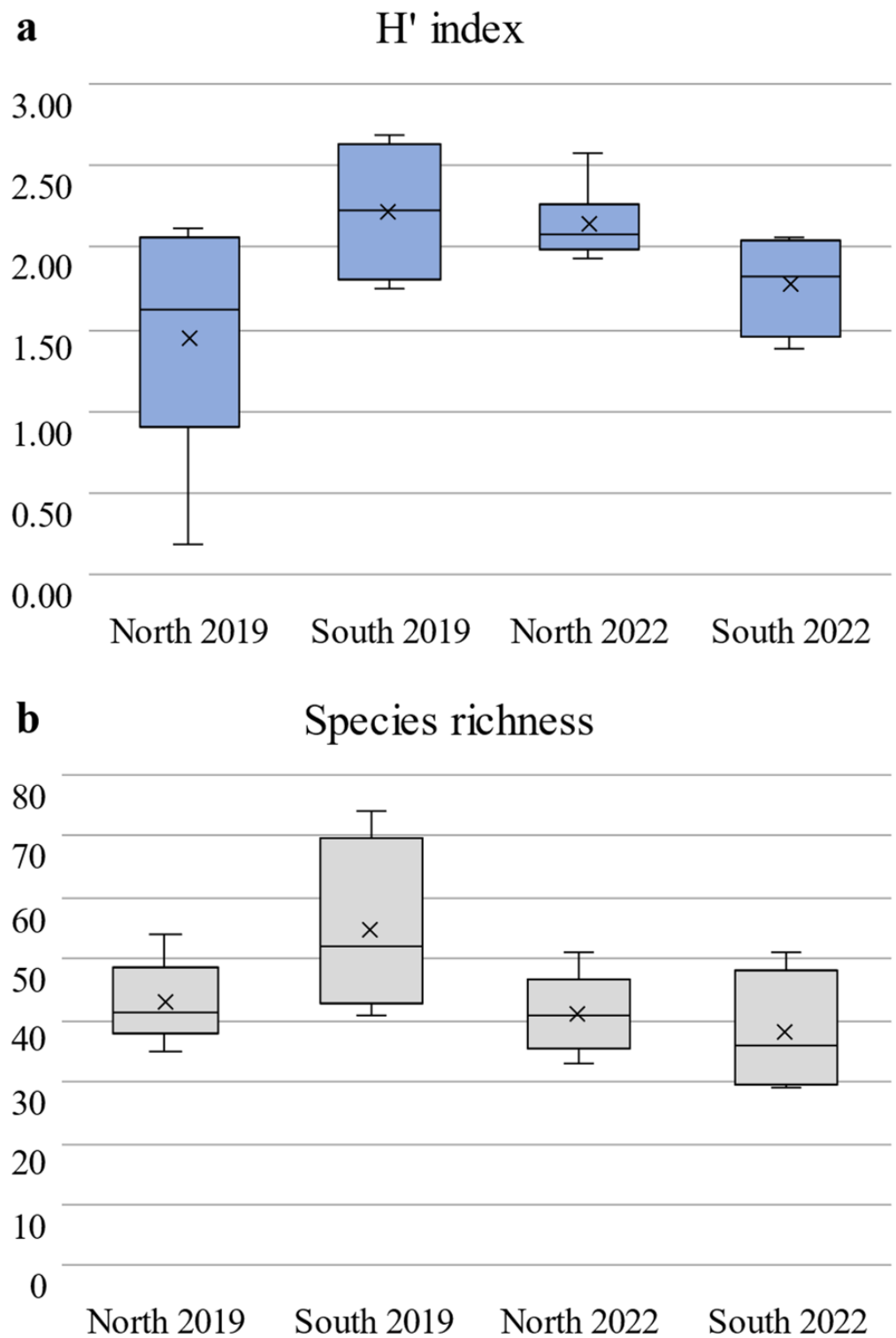
Figure 5. Box plots of diversity of zooplankton samples from 2019 and 2022, expressed as (**a**) H$'$ diversity index and (**b**) species richness for northern and southern sub-areas for each year. In the box plots, interquartile ranges are shown; black lines represent medians; crosses mark the mean values; and upper and lower whiskers represent max and min.
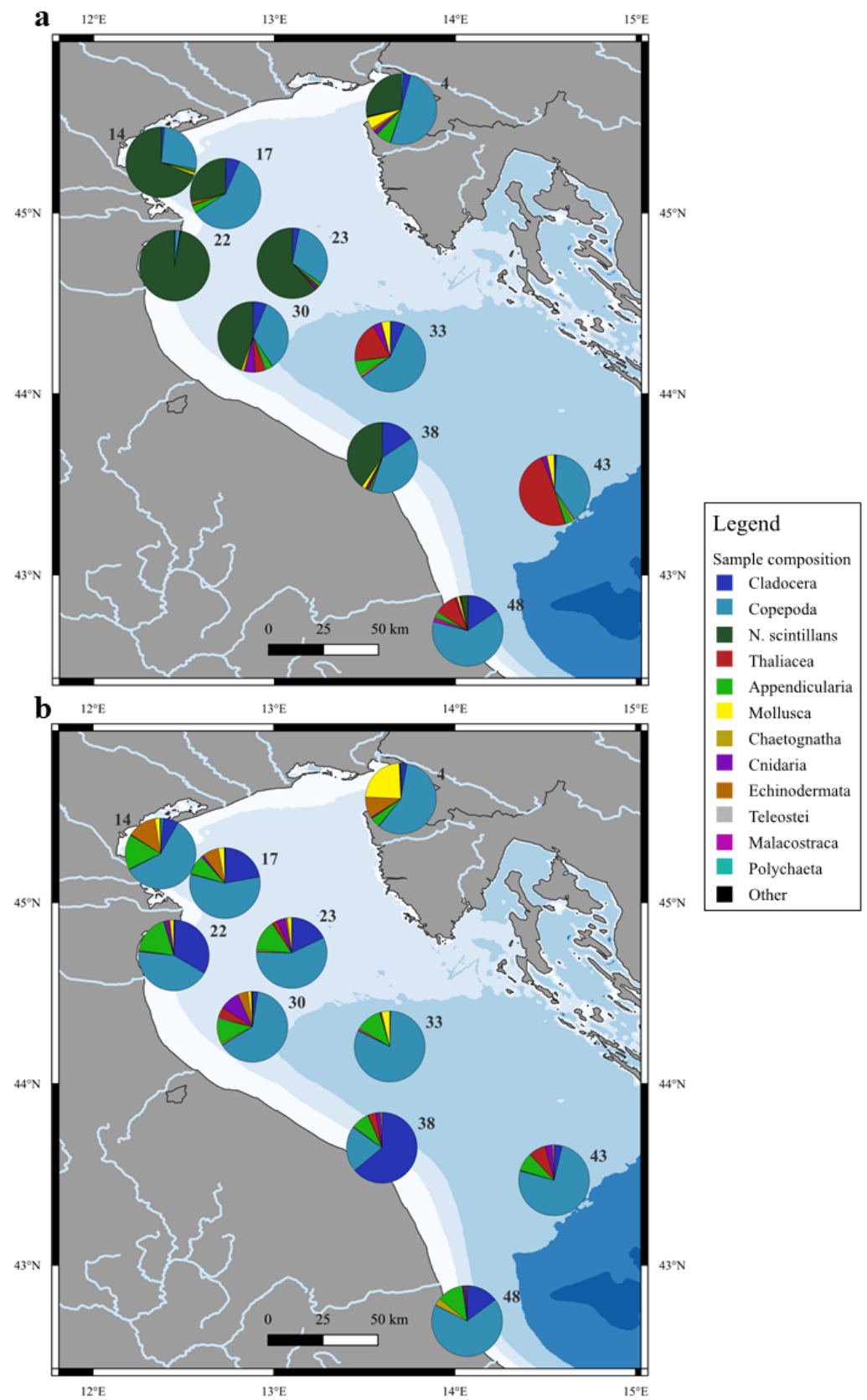
Figure 6. Pie charts of relative abundance (individuals per m^2) of organisms identified from the zooplankton analysis in (**a**) 2019 and (**b**) 2022.

In samples from 2022 (Table S7 in Supplementary Materials), on the other hand, *N. scintillans* was completely absent, and relative abundance was dominated by copepods in all stations, except station 38, where cladocerans made a higher contribution (Figure 5b). Among small copepods, *Acartia* sp. and *Oithona* sp. were less abundant, while small unidentified calanoids had a higher share of the total count. Large copepods also had some differences, with *Calanus helgolandicus* being more abundant, while *Temora stylifera* was not found in the examined samples. *Pseudodiaptomus marinus* was very rare, as it had only a minimal presence in station 30. Cladocerans were the second most abundant taxon, with some differences in their composition: *Evadne nordmanni* disappeared in 2022, and *Podon intermedius* and *Pleopis polyphemoides* faced a clear reduction; meanwhile, *Pseudoevadne tergestina*, *Penilia avirostris*, and *Evadne spinifera* were much more abundant. The presence of gelatinous zooplankton was also extremely pronounced, with larvaceans of the genus *Oikopleura* being the main contributors to total abundance. *Muggiaea* sp., anthomedusae, and Chaetognatha were also present in higher numbers compared to 2019. On the contrary, thaliaceans were determined to be less abundant in 2022, as small doliolids were much less numerous. However, a concurrent increase in large salps, mainly *Salpa fusiformis* and *Thalia democratica*, was recorded, particularly in station 23, where they were the main contributors to total biomass. Regarding meroplankton, a spike in abundance was registered for veliger larvae and ophioplutei, especially in northern samples (Figure 7).
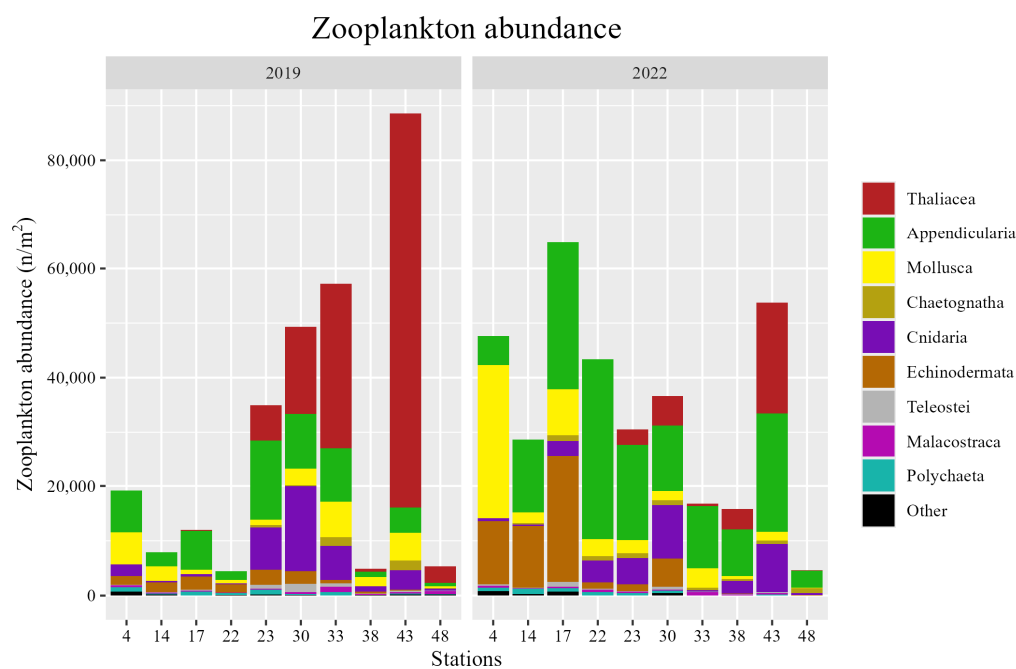

Figure 7. Bar plot of zooplankton abundance (individuals per m^2) of less represented taxa.

Multivariate PERMANOVA analyses of relative abundance (Table S3 in Supplementary Materials) uncovered the presence of significant variations of the zooplankton community between the examined years both over the whole area and within each sub-area. However, the nMDS plot (Figure 8a) mostly dispersed samples according to their geographic distribution rather than their sampling year. Such a degree of difference was also confirmed by the cluster analysis (Figure 8b), wherein three main groups were identified: (i) north inshore stations, which actually also included sample 38_2019 from the southern area and samples 17_2019 and 17_2022 from an offshore station; (ii) north offshore stations, which included the southern inshore sample 38_2022; and (iii) southern offshore samples. Station 48 was an outlier, differing quite a lot from the others.
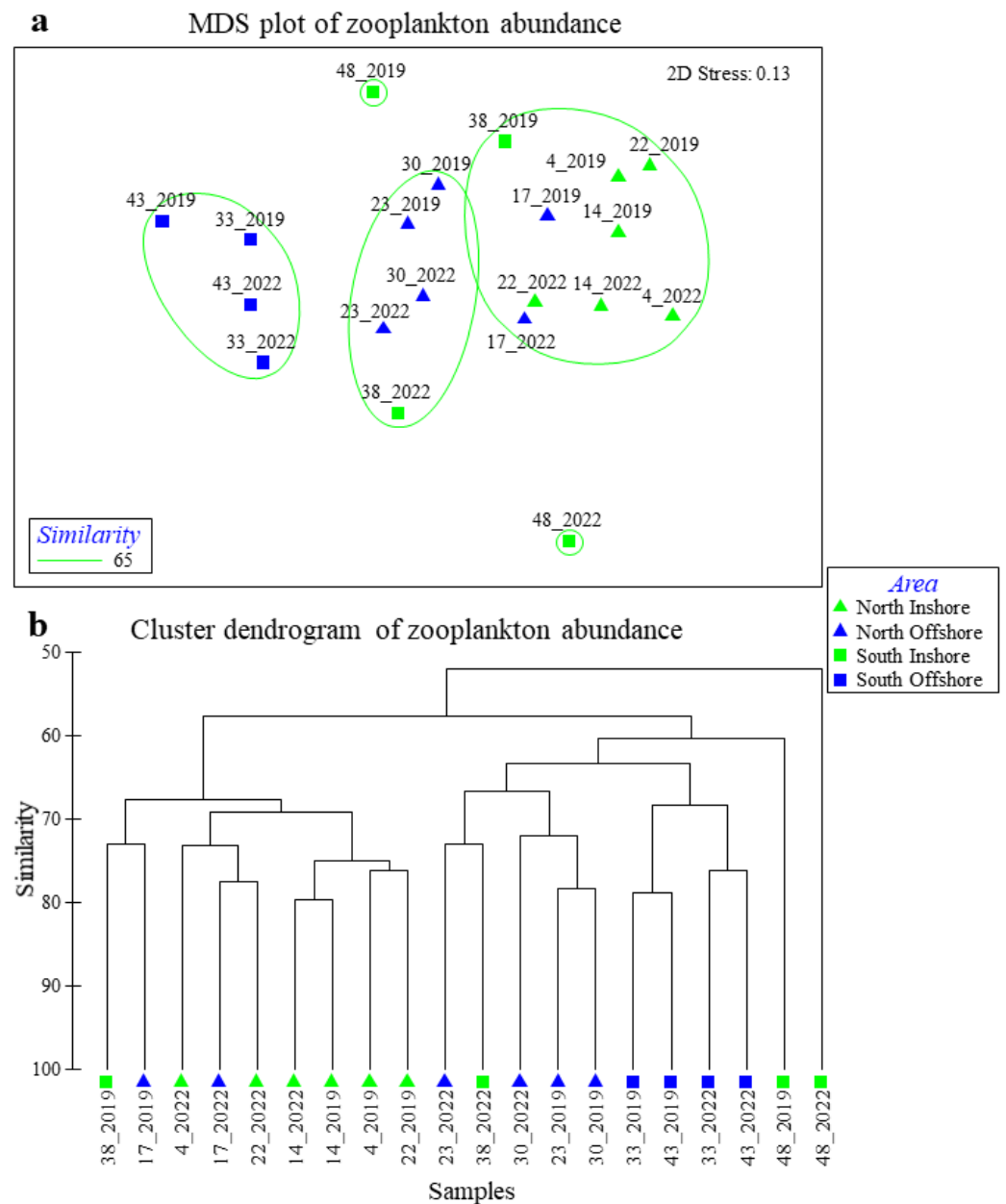
Figure 8. Results from the (**a**) nMDS and (**b**) hierarchical cluster analysis on the multivariate matrix of zooplankton abundance. The overlayed clusters in (**a**) are groups identified by (**b**) at 65% Bray–Curtis similarity.

Results from the SIMPER analysis (Table S4 in Supplementary Materials) evidenced that the main features responsible for the temporal differences in examined samples are the high abundance of *Noctiluca scintillans* and *Evadne nordmanni*, which could only be found in samples from 2019; the increase in *Calanus helgolandicus*, *Centropages ponticus*, Clauso-Paracalanidae, ophioplutei, *Penilia avirostris,* and *Pseudevadne tergestina,* registered in 2022; and a concurrent reduction in *Pleopis poliphemoides* and *Doliolina muelleri*.

3.3. Influence of Environmental Parameters on the Plankton Community

Prior to the DISTLM run, environmental variables were tested for collinearity, revealing a strong correlation between temperature and oxygen saturation and between salinity and fluorescence (R > 0.7). Therefore, the DISTLM analysis was performed on the abundance matrix, with salinity and temperature as environmental variables. The best solution for the DISTLM analysis had both salinity and temperature as explanatory

variables, accounting, respectively, for 22% and 11.4% of the total variance (Table S5 in Supplementary Materials).

Spearman's correlation analysis (Table 2) found a strong negative correlation of both abundance and biomass with temperature, as copepods, the most abundant group of metazooplankton, showed the same trend. Species richness also followed this pattern. Conversely, *N. scintillans* had a significant negative correlation with salinity, while thaliaceans had a positive correlation with the same variable. A weak but significant negative correlation was also noted for *N. scintillans* with the H′ diversity index.

Table 2. Results of the Spearman's correlation analysis on the matrix of abundant zooplankton species, diversity, and environmental variables. The top right values are resulting correlation coefficients, with significant pairs ($p < 0.05$) marked in red. The bottom left cells show corresponding *p*-values. Temp = temperature, Tot abund = total abundance, Tot biom = total biomass, H′ = H′ diversity index, and S = species richness.

	Temp	Salinity	Tot Abund	Tot Biom	*N. scintillans*	H′	S	Cladocera	Copepoda	Thaliacea
Temp		−0.402	−0.617	−0.675	−0.280	0.086	−0.515	−0.050	−0.672	−0.454
Salinity	0.079		-0.174	0.135	−0.606	0.244	0.331	−0.226	0.269	0.612
Tot abund	0.004	0.462		0.805	0.495	−0.292	0.399	0.408	0.654	0.094
Tot biom	0.001	0.569	<0.001		0.216	0.020	0.439	0.374	0.699	0.337
N. scintillans	0.232	0.005	0.026	0.361		−0.469	0.148	0.038	0.016	−0.058
H′	0.719	0.301	0.212	0.935	0.037		0.250	−0.099	0.128	0.220
S	0.020	0.154	0.081	0.053	0.532	0.288		−0.020	0.504	0.646
Cladocera	0.835	0.339	0.075	0.104	0.874	0.677	0.935		0.373	0.106
Copepoda	0.001	0.251	0.002	0.001	0.945	0.591	0.023	0.105		0.324
Thaliacea	0.044	0.004	0.695	0.146	0.809	0.352	0.002	0.655	0.164	

4. Discussion

Our work was a preliminary attempt to analyze the interannual variation of the early-summer mesozooplanktonic community in the North Adriatic Sea, comparing two years with very different climatic and environmental features and investigating the link between biotic and abiotic components. Results from the analyses performed on environmental variables evidenced the effect of the 2022 climatic anomaly on physical parameters and primary productivity at sea. The increase in temperature values was only significant in stations from the northern sub-area, where the lower bottom depth favored the heat transfer over the whole water column [46]. Meanwhile, the effect of the reduction in river run-off experienced during 2022 was quite evident in inshore stations, as salinity values were significantly higher and fluorescence values were significantly lower. The negative correlation between these parameters confirmed the role of river discharge on nutrient availability [47,48], which can positively influence the Adriatic productivity through a bottom-up mechanism [49]. This phenomenon is particularly important in the western coastal area, where a decreasing trend in nutrient loads and general river input was linked to a shift towards oligotrophic conditions and to changes in the phytoplanktonic community [33,34,47,50]. By comparing the surface chlorophyll concentration from satellite data (Figure 9) recorded before the sampling in station 22 (the closest to the Po River delta) in both 2019 and 2022, we can also conclude that the decrease in phytoplankton biomass is unlikely to have been caused by a shift in phenology, since the expected peak in phytoplankton standing stock did not occur in spring 2022.
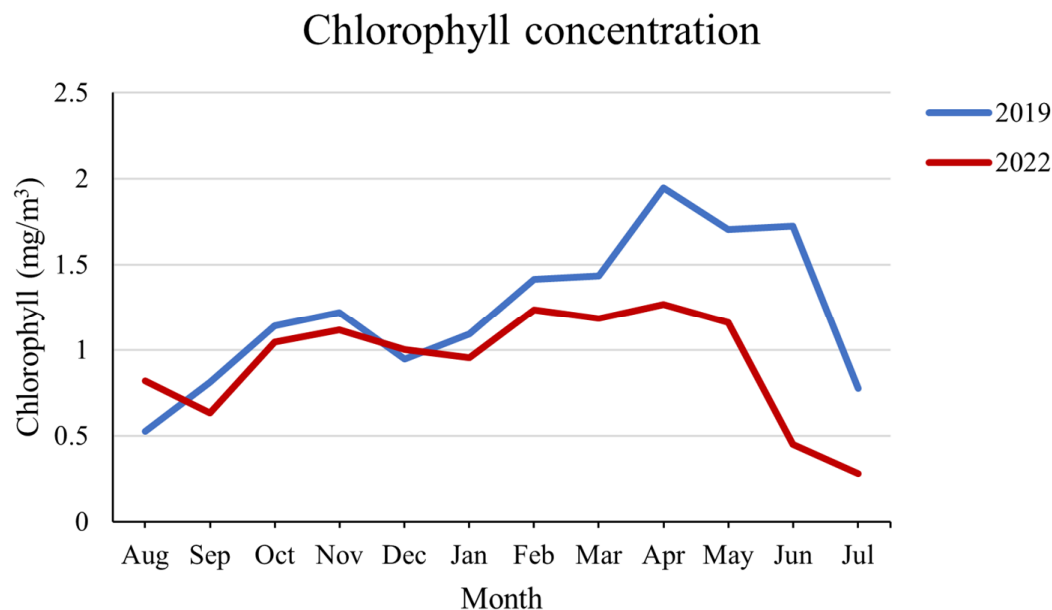
Chlorophyll concentration

Figure 9. Monthly mean chlorophyll concentration (mg/m^3) for the period before the survey in 2019 and 2022 in station 22 at 1 m depth. Data were taken from [51].

The PCA plot and the cluster grouping confirmed that inshore stations experienced larger variations in environmental conditions compared to offshore stations, where the water column is generally more stable and less influenced by coastal processes and continental inputs [46,52].

Mesozooplankton analysis allowed us to detect the community shift that happened in the North Adriatic Sea between 2019 and 2022. In both years, an increasing trend in both biomass and abundance is quite evident as samples approach the Po River area, confirming the importance of this zone for the productivity of the basin. However, neither biomass nor abundance differed significantly across years. This phenomenon is not entirely unexpected, as other authors have reported the uncoupling of zooplankton production with phytoplankton availability, pointing to the importance of other trophic dynamics, namely the microbial food web [53–56]. Even though total abundance and total biomass did not differ much across these years, species number faced a steep reduction, decreasing from 106 to 87 identified taxa. This reduction was stronger for southern samples, where we noticed the disappearance of several copepod and cnidarian species. In particular, many of the species that occurred in 2019 but not in 2022 were taxa more commonly identified in the deep waters of the South Adriatic, like *Diaixis pygmaea*, *Pareucalanus sewelli*, *Aetideus armatus*, *Eudoxoides spiralis*, and *Aglaura hemistoma* [57–60]. Therefore, the presence of these species in 2019 might stem from the advection of southern waters, which did not happen in 2022.

Relative abundance in 2019 was overwhelmed by *N. scintillans*, a heterotrophic dinoflagellate that can be responsible for large bloom events, called "red tides". These bloom events are quite common in the North Adriatic, typically from April to July [61]. This omnivorous organism can feed on bacteria, phytoplankton, detritus, protozoan, nauplii, and copepod and fish eggs [61]. In our samples, we also found some specimens containing *Pleopis polyphemoides*, *Evadne nordmanni*, and ostracods. The abundance of *N. scintillans* is usually linked to phytoplankton concentration and water column stability, as reported for East China Sea, Black Sea, open South Adriatic, and North Adriatic [62–64]. Our results confirmed the influence of primary productivity on *Noctiluca* cell concentration, which reached its peak in the northern sub-area, directly influenced by the Po River discharge in which low salinity values can increase water stratification in summer, while nutrient input from land fuels the formation of phytoplanktonic blooms [33,46,47]. The disappearance of *Noctiluca* in 2022 might be related to the concurrent increase in some cladoceran and

copepod species, which might have been negatively affected by food competition and direct predation from this dinoflagellate [61,65–67]. Indeed, even if no significant correlation was found for copepods or cladocerans with dinoflagellates, we did notice a low presence of both taxa in the sample where *Noctiluca* abundance was higher.

Marine cladocerans are capable of parthenogenetic reproduction, have short generation times, and can increase the number of individuals in an area rapidly, causing "blooms" very similar to those observed for phytoplankton, when environmental conditions are favorable [68]. The changes in environmental and trophic parameters registered between 2019 and 2022 might therefore be connected to the altered composition of the cladoceran community. *Evadne nordmanni*, which is generally considered a cold-water species [68,69], disappeared from 2022 samples, concurrently with the increase in temperature in the northern sub-area. Meanwhile, the decrease observed for *Pleopis poliphemoides* fitted well with the observed increase in salinity, since this is a typically estuarine species and can be found in open sea only when less saline water spreads offshore [69]. On the other hand, *Penilia avirostris* and *Pseudevadne tergestina* had an opposite trend, increasing their presence in the hot waters of the coastal areas in 2022. This observation confirmed the findings of [69,70], who classified these species in the "warm-water" group.

Doliolids seemed to prefer opposite conditions compared to *Noctiluca*, being more abundant in colder and saltier offshore stations. They have complex life cycles, with obligatory alternation of sexual and asexual generations, which means that they are able to respond to favorable conditions by producing offspring quickly, blooming at a speed comparable to that of phytoplankton [71]. The environmental parameters we registered in open water areas did not show significant differences; therefore, the reduction observed in doliolids in our samples cannot be readily attributed to changes in the analyzed environmental conditions. The distribution of thaliaceans appears often patchy and hard to predict, and the hydrodynamic condition of the area, water column stability, phytoplankton composition, and wind stress may also be important factors in bloom development [72,73]. The decrease in doliolid abundance might also be responsible for the disappearance of sapphirinid copepods, which are known for feeding on pelagic tunicates [74].

Copepods faced a general increase in abundance in 2022, particularly in some herbivorous or mixtivorous species, like *Centropages ponticus*, *Calanus helgolandicus*, and Clauso-Paracalanidae [35,75,76]. The enhanced abundance of these primary consumers, despite the concurrent decrease in phytoplankton biomass, might be related to the decrease in competing herbivorous blooming species, i.e., *Noctiluca* in the northern sub-area and doliolids in the southern sub-area, which are known for easily monopolizing access to trophic resources [61,77].

Overall, the mesozooplankton community registered in 2019 was quite similar to the situation found by [35] in June 1996, when abundance was dominated by copepods and cladocerans (49 and 22%, respectively, of the total abundance), followed by doliolids, *Noctiluca*, siphonophores, and larvae of invertebrates. On the other hand, the 2022 shift in environmental conditions caused a deviation from the previously observed situation, with the disappearance of *Noctiluca* and a steep reduction in doliolids. This shift might also be responsible for a change in zooplankton phenology, altering the normal pattern of zooplankton development. However, a long-term monitoring is needed to understand seasonal trends in the mesozooplanctonic community.

The sample groupings identified by both nMDS and hierarchical cluster analyses confirmed the previous findings for the zooplankton community in the study area [35,59,78], which is usually divided into three main geographic groups:

- a coastal community with few abundant species like *Acartia clausi*, *Penilia avirostris*, and *Paracalanus parvus*, characterized by the direct influence of riverine inputs; this group also included station 17 from the offshore area directly in front of the Po River delta, testifying the offshore spreading of the low-density coastal water mass [11];
- a neritic community, similar to the coastal one but with a higher contribution from *Calanus helgolandicus*, *Temora longicornis*, and gelatinous zooplankton; sample 38_2022

was also in this group, probably because the change in environmental variables registered in 2022 favored species that thrive in presence of higher salinity and lower chlorophyll values;

- an "oceanic" community, characterized by an increase in species from deep areas like *Pareuchaeta hebes*, *Nannocalanus minor*, and *Nanomia bijuga.*

The spatial segregation also fitted well with the identified pattern of environmental drivers, since salinity (together with chlorophyll concentration) and temperature (together with oxygen saturation) both figured as significant factors shaping the presence and abundance of Adriatic plankton species and highlighted the importance of riverine inputs for the distribution of the zooplankton community. Moreover, in both years, plankton diversity in station 48 figured as an outlier, differing from the others. This station is indeed the most southern and the shallowest, characterized by the highest temperature and the lowest oxygen concentration. These extreme conditions might be the cause of the lower level of similarity registered in the cluster analysis. Finally, fluorescence was much lower in 2022 at the same station, which might explain the interannual differences in the local community's composition.

The ecological effect that the zooplankton shift registered in June 2022 might have had is hard to predict, as many major components of the plankton community decreased, while others increased. The presence of large quantities of *Noctiluca scintillans* could definitely have negative effects on other zooplankters [61,65–67], but it might also be favorable for those organisms that can prey on the protist. Studying the connection between athecate dinoflagellates and higher trophic levels is not as easy as for other unicellular marine organisms because they lack hard structures that are preserved in gut contents and are readily digested [79,80]. However, some authors did report the use of *N. scintillans* as prey for large copepods, fish larvae, crab larvae, and hydromedusae [81]. A similar effect could also be true for doliolids, which are known to be a trophic source of epi- and mesopelagic fishes, copepods, pelagic polychaetes, and hydromedusae [82]. Moreover, a large proportion of these thaliaceans are not consumed and usually sink to the bottom, together with their fecal pellets, where they can fuel the rich benthic community of the Northern Adriatic [82–84]. On the other hand, copepods and cladocerans, which increased in 2022, might have had a key role in the pelagic trophic web, as they are known to be the preferred food of many important pelagic species like sardine, sprat, Atlantic horse mackerel, and Mediterranean horse mackerel [5,85,86].

5. Conclusions

This study is a first attempt to analyze the effect that short-term climatic anomalies can have on environmental conditions at sea and consequently on the zooplankton community in the Northern Adriatic Sea. Even though the time and spatial extent of this study are quite limited, our work highlighted the community changes that happened in June in the mesozooplanktonic community between the analyzed years, registering a shift from a *Noctiluca*-dominated assemblage to a crustacean-dominated one and showing how some species thrived while others suffered in a modified environment. Our findings confirmed the influence of river inputs and temperature on the Adriatic community's distribution and composition, highlighting how climate-driven changes could have unpredictable effects on the whole Adriatic ecosystem. Therefore, more studies on a broader time scale are necessary to better understand the influence of climate change on the zooplankton community and the role of the main planktonic components in the Adriatic trophic web.

References

1. Sieburth, J.M.; Smetacek, V.; Lenz, J. Pelagic Ecosystem Structure: Heterotrophic Compartments of the Plankton and Their Relationship to Plankton Size Fractions. *Limnol. Oceanogr.* **1978**, *23*, 1256–1263. [CrossRef]
2. Hatton, I.A.; Heneghan, R.F.; Bar-On, Y.M.; Galbraith, E.D. The Global Ocean Size Spectrum from Bacteria to Whales. *Sci. Adv.* **2021**, *7*, eabh3732. [CrossRef]
3. Heneghan, R.F.; Everett, J.D.; Blanchard, J.L.; Sykes, P.; Richardson, A.J. Climate-Driven Zooplankton Shifts Cause Large-Scale Declines in Food Quality for Fish. *Nat. Clim. Chang.* **2023**, *13*, 470–477. [CrossRef]
4. Lomartire, S.; Marques, J.C.; Gonçalves, A.M.M. The Key Role of Zooplankton in Ecosystem Services: A Perspective of Interaction between Zooplankton and Fish Recruitment. *Ecol. Indic.* **2021**, *129*, 107867. [CrossRef]
5. Fanelli, E.; Da Ros, Z.; Menicucci, S.; Malavolti, S.; Biagiotti, I.; Canduci, G.; De Felice, A.; Leonori, I. The Pelagic Food Web of the Western Adriatic Sea: A Focus on the Role of Small Pelagics. *Sci. Rep.* **2023**, *13*, 14554. [CrossRef]
6. Borrell, A.; Gazo, M.; Aguilar, A.; Raga, J.A.; Degollada, E.; Gozalbes, P.; García-Vernet, R. Niche Partitioning amongst Northwestern Mediterranean Cetaceans Using Stable Isotopes. *Prog. Oceanogr.* **2021**, *193*, 102559. [CrossRef]
7. Peduzzi, P.; Herndl, G.J. Zooplankton Activity Fueling the Microbial Loop: Differential Growth Response of Bacteria from Oligotrophic and Eutrophic Waters. *Limnol. Oceanogr.* **1992**, *37*, 1087–1092. [CrossRef]
8. Calbet, A.; Saiz, E. The Ciliate-Copepod Link in Marine Ecosystems. *Aquat. Microb. Ecol.* **2005**, *38*, 157–167. [CrossRef]

9. Ruhl, H.A.; Smith, K.L. Shifts in Deep-Sea Community Structure Linked to Climate and Food Supply. *Science* **2004**, *305*, 513–515. [CrossRef]
10. Jónasdóttir, S.H.; Visser, A.W.; Richardson, K.; Heath, M.R. Seasonal Copepod Lipid Pump Promotes Carbon Sequestration in the Deep North Atlantic. *Proc. Natl. Acad. Sci. USA* **2015**, *112*, 12122–12126. [CrossRef]
11. Russo, A.; Artegiani, A. Adriatic Sea Hydrography. *Sci. Mar.* **1996**, *60*, 33–43.
12. Marini, M.; Bombace, G.; Iacobone, G. *Il Mare Adriatico e Le Sue Risorse*; Carlo Saladino Editore: Palermo, Italy, 2017; p. 267.
13. Calì, F.; Stranci, F.; La Mesa, M.; Mazzoldi, C.; Arneri, E.; Santojanni, A. Whiting (Merlangius Merlangus) Grows Slower and Smaller in the Adriatic Sea: New Insights from a Comparison of Two Populations with a Time Interval of 30 Years. *Fishes* **2023**, *8*, 341. [CrossRef]
14. CIESM. *Climate Warming and Related Changes in Mediterranean Marine Biota*; Workshop Monographs; CIESM Publisher: Monaco, Monaco, 2008.
15. García-Monteiro, S.; Sobrino, J.A.; Julien, Y.; Sòria, G.; Skokovic, D. Surface Temperature Trends in the Mediterranean Sea from MODIS Data during Years 2003–2019. *Reg. Stud. Mar. Sci.* **2022**, *49*, 102086. [CrossRef]
16. Giani, M.; Djakovac, T.; Degobbis, D.; Cozzi, S.; Solidoro, C.; Umani, S.F. Recent Changes in the Marine Ecosystems of the Northern Adriatic Sea. *Estuar. Coast. Shelf Sci.* **2012**, *115*, 1–13. [CrossRef]
17. Ben Rais Lasram, F.; Guilhaumon, F.; Albouy, C.; Somot, S.; Thuiller, W.; Mouillot, D. The Mediterranean Sea as a 'Cul-de-Sac' for Endemic Fishes Facing Climate Change. *Glob. Chang. Biol.* **2010**, *16*, 3233–3245. [CrossRef]
18. De Felice, A.; Iglesias, M.; Saraux, C.; Bonanno, A.; Tičina, V.; Leonori, I.; Ventero, A.; Hattab, T.; Barra, M.; Gašparević, D.; et al. Environmental Drivers Influencing the Abundance of Round Sardinella (Sardinella Aurita) and European Sprat (Sprattus Sprattus) in Different Areas of the Mediterranean Sea. *Mediterr. Mar. Sci.* **2021**, *22*, 812. [CrossRef]
19. Mariotti, A.; Struglia, M.V.; Zeng, N.; Lau, K.-M. The Hydrological Cycle in the Mediterranean Region and Implications for the Water Budget of the Mediterranean Sea. *J. Clim.* **2002**, *15*, 1674–1690. [CrossRef]
20. Caloiero, T.; Caloiero, P.; Frustaci, F. Long-term Precipitation Trend Analysis in Europe and in the Mediterranean Basin. *Water Environ. J.* **2018**, *32*, 433–445. [CrossRef]
21. Appiotti, F.; Krželj, M.; Russo, A.; Ferretti, M.; Bastianini, M.; Marincioni, F. A Multidisciplinary Study on the Effects of Climate Change in the Northern Adriatic Sea and the Marche Region (Central Italy). *Reg. Environ. Chang.* **2014**, *14*, 2007–2024. [CrossRef]
22. Coppola, E.; Verdecchia, M.; Giorgi, F.; Colaiuda, V.; Tomassetti, B.; Lombardi, A. Changing Hydrological Conditions in the Po Basin under Global Warming. *Sci. Total Environ.* **2014**, *493*, 1183–1196. [CrossRef]
23. Soana, E.; Gervasio, M.P.; Granata, T.; Colombo, D.; Castaldelli, G. Climate Change Impacts on Eutrophication in the Po River (Italy): Temperature-Mediated Reduction in Nitrogen Export but No Effect on Phosphorus. *J. Environ. Sci.* **2023**, *143*, 148–163. [CrossRef]
24. Marini, M.; Grilli, F. The Role of Nitrogen and Phosphorus in Eutrophication of the Northern Adriatic Sea: History and Future Scenarios. *Appl. Sci.* **2023**, *13*, 9267. [CrossRef]
25. Sani, T.; Marini, M.; Campanelli, A.; Machado Toffolo, M.; Goffredo, S.; Grilli, F. Evolution of Freshwater Runoff in the Western Adriatic Sea over the Last Century. *Environments* **2024**, *11*, 22. [CrossRef]
26. Montanari, A.; Nguyen, H.; Rubinetti, S.; Ceola, S.; Galelli, S.; Rubino, A.; Zanchettin, D. Why the 2022 Po River Drought Is the Worst in the Past Two Centuries. *Sci. Adv.* **2023**, *9*, eadg8304. [CrossRef]
27. Copernicus Climate Change Service (C3S). European State of the Climate 2022. 2023. Available online: https://climate.copernicus.eu/ESOTC/2022 (accessed on 15 December 2023).
28. Garrabou, J.; Gómez-Gras, D.; Medrano, A.; Cerrano, C.; Ponti, M.; Schlegel, R.; Bensoussan, N.; Turicchia, E.; Sini, M.; Gerovasileiou, V.; et al. Marine Heatwaves Drive Recurrent Mass Mortalities in the Mediterranean Sea. *Glob. Chang. Biol.* **2022**, *28*, 5708–5725. [CrossRef]
29. Zanchettin, D. Monthly Discharge of Po River at Pontelagoscuro [Data Set]. Zenodo, 2022. Available online: www.zenodo.org/records/7225699 (accessed on 15 December 2023).
30. Druon, J.-N.; Hélaouët, P.; Beaugrand, G.; Fromentin, J.-M.; Palialexis, A.; Hoepffner, N. Satellite-Based Indicator of Zooplankton Distribution for Global Monitoring. *Sci. Rep.* **2019**, *9*, 4732. [CrossRef]
31. Degobbis, D.; Gilmartin, M. Nitrogen, Phosphorus, and Biogenic Silicon Budgets for the Northern Adriatic Sea. *Oceanol. Acta* **1990**, *13*, 31–45.
32. Zavatarelli, M.; Pinardi, N. The Adriatic Sea Modelling System: A Nested Approach. *Ann. Geophys.* **2003**, *21*, 345–364. [CrossRef]
33. Mozetič, P.; Solidoro, C.; Cossarini, G.; Socal, G.; Precali, R.; Francé, J.; Bianchi, F.; De Vittor, C.; Smodlaka, N.; Fonda Umani, S. Recent Trends Towards Oligotrophication of the Northern Adriatic: Evidence from Chlorophyll a Time Series. *Estuaries Coasts* **2010**, *33*, 362–375. [CrossRef]
34. Totti, C.; Romagnoli, T.; Accoroni, S.; Coluccelli, A.; Pellegrini, M.; Campanelli, A.; Grilli, F.; Marini, M. Phytoplankton Communities in the Northwestern Adriatic Sea: Interdecadal Variability over a 30-Years Period (1988–2016) and Relationships with Meteoclimatic Drivers. *J. Mar. Syst.* **2019**, *193*, 137–153. [CrossRef]
35. Guglielmo, L.; Sidoti, O.; Granata, A.; Zagami, G. Distribution, Biomass and Ecology of Meso-Zooplankton in the Northern Adriatic Sea. *Chem. Ecol.* **2002**, *18*, 107–115. [CrossRef]

36. Aubry, F.B.; Cossarini, G.; Acri, F.; Bastianini, M.; Bianchi, F.; Camatti, E.; De Lazzari, A.; Pugnetti, A.; Solidoro, C.; Socal, G. Plankton Communities in the Northern Adriatic Sea: Patterns and Changes over the Last 30 Years. *Estuar. Coast. Shelf Sci.* **2012**, *115*, 125–137. [CrossRef]

37. Camatti, E.; Comaschi, A.; De Olazabal, A.; Fonda Umani, S. Annual Dynamics of the Mesozooplankton Communities in a Highly Variable Ecosystem (North Adriatic Sea, Italy). *Mar. Ecol.* **2008**, *29*, 387–398. [CrossRef]

38. UNEP-MAP-RAC/SPA; Farrugio, H.; Soldo, A. *Adriatic Sea: Status and Conservation of Fisheries*; Cebrian, D., Requena, S., Eds.; RAC/SPA: Tunis, Tunisia, 2015.

39. Penna, N.; Capellacci, S.; Ricci, F. The Influence of the Po River Discharge on Phytoplankton Bloom Dynamics along the Coastline of Pesaro (Italy) in the Adriatic Sea. *Mar. Pollut. Bull.* **2004**, *48*, 321–326. [CrossRef]

40. Degobbis, D.; Fonda-Umani, S.; Franco, P.; Malej, A.; Precali, R.; Smodlaka, N. Changes in the Northern Adriatic Ecosystem and the Hypertrophic Appearance of Gelatinous Aggregates. *Sci. Total Environ.* **1995**, *165*, 43–58. [CrossRef]

41. Leonori, I.; Tičina, V.; Giannoulaki, M.; Hattab, T.; Iglesias, M.; Bonanno, A.; Costantini, I.; Canduci, G.; Machias, A.; Ventero, A.; et al. History of Hydroacoustic Surveys of Small Pelagic Fish Species in the European Mediterranean Sea. *Mediterr. Mar. Sci.* **2021**, *22*, 751–768. [CrossRef]

42. MEDIAS Steering Committee. Common Protocol for the MEDiterranean International Acoustic Survey (MEDIAS). Available online: http://www.medias-project.eu/ (accessed on 15 December 2023).

43. Trenkel, V.; Ressler, P.; Jech, M.; Giannoulaki, M.; Taylor, C. Underwater Acoustics for Ecosystem-Based Management: State of the Science and Proposals for Ecosystem Indicators. *Mar. Ecol. Prog. Ser.* **2011**, *442*, 285–301. [CrossRef]

44. Clarke, K.R.; Gorley, R.N. *Primer V6: User Manual/Tutorial*; PRIMER-e: Auckland, New Zealand, 2006.

45. Anderson, M.; Gorley, R.N.; Clarke, K. *PERMANOVA+ for Primer: Guide to Software and Statistical Methods*; PRIMER-e: Auckland, New Zealand, 2008.

46. Artegiani, A.; Paschini, E.; Russo, A.; Bregant, D.; Raicich, F.; Pinardi, N. The Adriatic Sea General Circulation. Part I: Air–Sea Interactions and Water Mass Structure. *J. Phys. Oceanogr.* **1997**, *27*, 1492–1514. [CrossRef]

47. Ricci, F.; Capellacci, S.; Campanelli, A.; Grilli, F.; Marini, M.; Penna, A. Long-Term Dynamics of Annual and Seasonal Physical and Biogeochemical Properties: Role of Minor River Discharges in the North-Western Adriatic Coast. *Estuar. Coast. Shelf Sci.* **2022**, *272*, 107902. [CrossRef]

48. Gilmartin, M.; Degobbis, D.; Revelante, N.; Smodlaka, N. The Mechanism Controlling Plant Nutrient Concentrations in the Northern Adriatic Sea. *Int. Rev. Gesamten Hydrobiol. Hydrogr.* **1990**, *75*, 425–445. [CrossRef]

49. Mozetič, P.; Francé, J.; Kogovšek, T.Š.; Talaber, I.; Malej, A. Plankton Trends and Community Changes in a Coastal Sea (Northern Adriatic): Bottom-up vs. Top-down Control in Relation to Environmental Drivers. *Estuar. Coast. Shelf Sci.* **2012**, *115*, 138–148. [CrossRef]

50. Casabianca, S.; Capellacci, S.; Ricci, F.; Scardi, M.; Penna, A. A Phytoplankton Time Series in the Northwestern Adriatic Sea: Structure and Dynamics of the Assemblages in a Coastal Ecosystem. *Estuar. Coast. Shelf Sci.* **2022**, *278*, 108109. [CrossRef]

51. Teruzzi, A.; Di Biagio, V.; Feudale, L.; Bolzon, G.; Lazzari, P.; Salon, S.; Coidessa, G.; Cossarini, G. Mediterranean Sea Biogeochemical Reanalysis (CMEMS MED-Biogeochemistry, MedBFM3 System) (Version 1) [Data Set]. E.U. Copernicus Marine Service Information (CMEMS). 2021. Available online: https://data.marine.copernicus.eu/product/MEDSEA_MULTIYEAR_BGC_006_008/description?view=-&option=-&product_id=- (accessed on 15 December 2023).

52. Neri, F.; Romagnoli, T.; Accoroni, S.; Ubaldi, M.; Garzia, A.; Pizzuti, A.; Campanelli, A.; Grilli, F.; Marini, M.; Totti, C. Phytoplankton Communities in a Coastal and Offshore Stations of the Northern Adriatic Sea Approached by Network Analysis and Different Statistical Descriptors. *Estuar. Coast. Shelf Sci.* **2023**, *282*, 108224. [CrossRef]

53. Fonda Umani, S.; Milani, L.; Borme, D.; de Olazabal, A.; Parlato, S.; Precali, R.; Kraus, R.; Lučić, D.; Njire, J.; Totti, C.; et al. Inter-Annual Variations of Planktonic Food Webs in the Northern Adriatic Sea. *Sci. Total Environ.* **2005**, *353*, 218–231. [CrossRef]

54. Barausse, A.; Duci, A.; Mazzoldi, C.; Artioli, Y.; Palmeri, L. Trophic Network Model of the Northern Adriatic Sea: Analysis of an Exploited and Eutrophic Ecosystem. *Estuar. Coast. Shelf Sci.* **2009**, *83*, 577–590. [CrossRef]

55. Fuks, D.; Ivančić, I.; Najdek, M.; Lučić, D.; Njire, J.; Godrijan, J.; Marić, D.; Šilović, T.; Paliaga, P.; Blažina, M.; et al. Changes in the Planktonic Community Structure Related to Trophic Conditions: The Case Study of the Northern Adriatic Sea. *J. Mar. Syst.* **2012**, *96–97*, 95–102. [CrossRef]

56. Kamburska, L.; Fonda-Umani, S. From Seasonal to Decadal Inter-Annual Variability of Mesozooplankton Biomass in the Northern Adriatic Sea (Gulf of Trieste). *J. Mar. Syst.* **2009**, *78*, 490–504. [CrossRef]

57. Pestorić, B.; Drakulović, D.; Lučić, D.; Đorđević, N.; Joksimović, D. Zooplankton in Montenegrin Adriatic Offshore Waters. In *The Montenegrin Adriatic Coast: Marine Biology*; Joksimović, A., Đurović, M., Zonn, I.S., Kostianoy, A.G., Semenov, A.V., Eds.; Springer International Publishing: Cham, Switzerland, 2021; pp. 107–128, ISBN 978-3-030-77513-1.

58. Batistić, M.; Kršinić, F.; Jasprica, N.; Carić, M.; Viličić, D.; Lučić, D. Gelatinous Invertebrate Zooplankton of the South Adriatic: Species Composition and Vertical Distribution. *J. Plankton Res.* **2004**, *26*, 459–474. [CrossRef]

59. Fonda Umani, S.; Franco, P.; Ghirardelli, E.; Malej, A. Outline of Oceanography and the Plankton of the Adriatic Sea. In *Marine Eutrophication and Population Dynamics*; Colombo, G., Ferrari, I., Ceccherelli, V.U., Rossi, R., Eds.; Olsen & Olsen: Fredensburg, Denmark, 1992; pp. 347–365.

60. Miloslavić, M.; Lučić, D.; Njire, J.; Gangai, B.; Onofri, I.; Garić, R.; Žarić, M.; Miri Osmani, F.; Pestorić, B.; Nikleka, E.; et al. Zooplankton Composition and Distribution across Coastal and Offshore Waters off Albania (Southern Adriatic) in Late Spring. *Acta Adriat.* **2012**, *53*, 165–180.

61. Fonda Umani, S.; Beran, A.; Parlato, S.; Virgilio, D.; Zollet, T.; De Olazabal, A.; Lazzarini, B.; Cabrini, M. Noctiluca Scintillans MACARTNEY in the Northern Adriatic Sea: Long-Term Dynamics, Relationships with Temperature and Eutrophication, and Role in the Food Web. *J. Plankton Res.* **2004**, *26*, 545–561. [CrossRef]

62. Batistić, M.; Garić, R.; Jasprica, N.; Ljubimir, S.; Mikuš, J. Bloom of the Heterotrophic Dinoflagellate Noctiluca Scintillans (Macartney) Kofoid & Swezy, 1921 and Tunicates Salpa Fusiformis Cuvier, 1804 and Salpa Maxima Forskål, 1775 in the Open Southern Adriatic in 2009. *J. Mar. Biol. Assoc. United Kingd.* **2019**, *99*, 1049–1058. [CrossRef]

63. Mikaelyan, A.S.; Malej, A.; Shiganova, T.A.; Turk, V.; Sivkovitch, A.E.; Musaeva, E.I.; Kogovšek, T.; Lukasheva, T.A. Populations of the Red Tide Forming Dinoflagellate Noctiluca Scintillans (Macartney): A Comparison between the Black Sea and the Northern Adriatic Sea. *Harmful Algae* **2014**, *33*, 29–40. [CrossRef]

64. Sheng, L.; Jiang, Z.; Sun, Z.; Zhu, Y.; Zhai, H.; Ding, L.; Tong, M.; Chen, J.; Chen, Q.; Zeng, J. Noctiluca Scintillans Distribution Largely Regulated by Phytoplankton Biomass in the East China Sea and Southern Yellow Sea. *Front. Mar. Sci.* **2022**, *9*, 899334. [CrossRef]

65. Ollevier, A.; Mortelmans, J.; Aubert, A.; Deneudt, K.; Vandegehuchte, M.B. Noctiluca Scintillans: Dynamics, Size Measurements and Relationships With Small Soft-Bodied Plankton in the Belgian Part of the North Sea. *Front. Mar. Sci.* **2021**, *8*, 777999. [CrossRef]

66. Yılmaz, İ.N.; Okusˌ, E.; Yüksek, A. Evidences for Influence of a Heterotrophic Dinoflagellate (Noctiluca Scintillans) on Zooplankton Community Structure in a Highly Stratified Basin. *Estuar. Coast. Shelf Sci.* **2005**, *64*, 475–485. [CrossRef]

67. Quevedo, M.; Gonzalez-Quiros, R.; Anadon, R. Evidence of Heavy Predation by Noctiluca Scintillans on Acartia Clausi (Copepoda) Eggs off the Central Cantabrian Coast (NW Spain). *Oceanol. Acta* **1999**, *22*, 127–131. [CrossRef]

68. Kodama, T.; Ohshimo, S.; Tanaka, H.; Ashida, H.; Kameda, T.; Tanabe, T.; Okazaki, M.; Ono, T.; Tanaka, Y. Abundance and Habitats of Marine Cladocerans in the Sea of Japan over Two Decades. *Prog. Oceanogr.* **2021**, *194*, 102561. [CrossRef]

69. Gieskes, W.W.C. Ecology of the Cladocera of the North Atlantic and the North Sea, 1960–1967. *Neth. J. Sea Res.* **1971**, *5*, 342–376. [CrossRef]

70. Killi, N. Spatio-Temporal Variation in the Distribution and Abundance of Marine Cladocerans in Relation to Environmental Factors in a Productive Lagoon (Güllük Bay, SW Aegean Sea, Turkey). *Oceanol. Hydrobiol. Stud.* **2020**, *49*, 374–382. [CrossRef]

71. Deibel, D.; Paffenhofer, G.-A. Predictability of Patches of Neritic Salps and Doliolids (Tunicata, Thaliacea). *J. Plankton Res.* **2009**, *31*, 1571–1579. [CrossRef]

72. Lavaniegos, B.E.; Ohman, M.D. Long-Term Changes in Pelagic Tunicates of the California Current. *Deep. Sea Res. Part II Top. Stud. Oceanogr.* **2003**, *50*, 2473–2498. [CrossRef]

73. Ménard, F.; Fromentin, J.-M.; Goy, J.; Dallot, S. Temporal Fluctuations of Doliolid Abundance in the Bay of Villefranche-Sur-Mer (Northwestern Mediterranean Sea). *Oceanol. Acta* **1997**, *20*, 106.

74. Takahashi, K.; Ichikawa, T.; Saito, H.; Kakehi, S.; Sugimoto, Y.; Hidaka, K.; Hamasaki, K. Sapphirinid Copepods as Predators of Doliolids: Their Role in Doliolid Mortality and Sinking Flux. *Limnol. Oceanogr.* **2013**, *58*, 1972–1984. [CrossRef]

75. Neffati, N.; Daly Yahia-Kefi, O.; Bonnet, D.; Carlotti, F.; Daly Yahia, M.N. Reproductive Traits of Two Calanoid Copepods: Centropages Ponticus and Temora Stylifera, in Autumn in Bizerte Channel. *J. Plankton Res.* **2013**, *35*, 80–96. [CrossRef]

76. Fanelli, E.; Menicucci, S.; Malavolti, S.; De Felice, A.; Leonori, I. Spatial Changes in Community Composition and Food Web Structure of Mesozooplankton across the Adriatic Basin (Mediterranean Sea). *Biogeosciences* **2022**, *19*, 1833–1851. [CrossRef]

77. Haskell, A. Modeling the Effects of Doliolids on the Plankton Community Structure of the Southeastern US Continental Shelf. *J. Plankton Res.* **1999**, *21*, 1725–1752. [CrossRef]

78. Stefanni, S.; Stanković, D.; Borme, D.; de Olazabal, A.; Juretić, T.; Pallavicini, A.; Tirelli, V. Multi-Marker Metabarcoding Approach to Study Mesozooplankton at Basin Scale. *Sci. Rep.* **2018**, *8*, 12085. [CrossRef]

79. Sullivan, L.J. Gut Evacuation of Larval Mnemiopsis Leidyi A. Agassiz (Ctenophora, Lobata). *J. Plankton Res.* **2010**, *32*, 69–74. [CrossRef]

80. Friedenberg, L.E.; Bollens, S.M.; Rollwagen-Bollens, G. Feeding Dynamics of Larval Pacific Herring (Clupea Pallasi) on Natural Prey Assemblages: The Importance of Protists. *Fish. Oceanogr.* **2012**, *21*, 95–108. [CrossRef]

81. Fock, H.O.; Greve, W. Analysis and Interpretation of Recurrent Spatio-Temporal Patterns in Zooplankton Dynamics: A Case Study on Noctiluca Scintillans (Dinophyceae) in the German Bight (North Sea). *Mar. Biol.* **2002**, *140*, 59–73. [CrossRef]

82. Takahashi, K.; Ichikawa, T.; Fukugama, C.; Yamane, M.; Kakehi, S.; Okazaki, Y.; Kubota, H.; Furuya, K. In Situ Observations of a Doliolid Bloom in a Warm Water Filament Using a Video Plankton Recorder: Bloom Development, Fate, and Effect on Biogeochemical Cycles and Planktonic Food Webs. *Limnol. Oceanogr.* **2015**, *60*, 1763–1780. [CrossRef]

83. Martin, B.; Koppelmann, R.; Kassatov, P. Ecological Relevance of Salps and Doliolids in the Northern Benguela Upwelling System. *J. Plankton Res.* **2016**, *39*, 290–304. [CrossRef]

84. Paffenhöfer, G.; Köster, M. Digestion of Diatoms by Planktonic Copepods and Doliolids. *Mar. Ecol. Prog. Ser.* **2005**, *297*, 303–310. [CrossRef]

85. Borme, D.; Legovini, S.; de Olazabal, A.; Tirelli, V. Diet of Adult Sardine Sardina Pilchardus in the Gulf of Trieste, Northern Adriatic Sea. *J. Mar. Sci. Eng.* **2022**, *10*, 1012. [CrossRef]

86. Da Ros, Z.; Fanelli, E.; Cassatella, S.; Biagiotti, I.; Canduci, G.; Menicucci, S.; De Felice, A.; Malavolti, S.; Leonori, I. Resource Partitioning among "Ancillary" Pelagic Fishes (*Scomber* spp., *Trachurus* spp.) in the Adriatic Sea. *Biology* **2023**, *12*, 272. [CrossRef]